# Theoretical and Experimental Study on Vibration of Cracked Shafts using Order Analysis

**M. Farahmandian***
Department of Mechanical Engineering,
East Azarbaijan Science and Research Branch,
Islamic Azad University, Tabriz, Iran
E-mail: mahdi.farahmandian@gmail.com
*Corresponding author

**M. H. Sadeghi**
Department of Mechanical Engineering,
University of Tabriz, Iran
E-mail: morteza@tabrizu.ac.ir

**Received: 7 May 2013, Revised: 15 July 2013, Accepted: 18 December 2013**

**Abstract:** In this paper, the effects of transverse cracks on rotating shaft are studied. According to earlier works, crack shaft failure decrease the critical speed of the shaft and also exhibit a nonlinear vibration behaviour leading to increases the amplitude of 1X and 2X harmonics (first and second order of rotational speed in torsional vibration). This suggests that the application of order analysis to be very effective. Moreover, vibrations arising from resonance frequencies of the system can be differentiated from other ones, by using this method. For this purpose in this article, first, un cracked and cracked shaft were mathematically modelled and numerical analysis were carried out to obtain the vibration response for both healthy and faulty shaft. Then order analysis method was applied on the vibration signals obtained from the model. Finally, an experiment was also carried out on a laboratory scale test rig to verify effectiveness of the order analysis in practice. The results indicate that the vibration orders arising from torsional vibration can be clearly sensed by the transducers installed on the supports which primarily measure the bending vibrations.

**Keywords:** Cracked Rotating Shaft, Fault Detection, Nonlinear Vibrations, Order Analysis

**Reference:** M. Farahmandian, M. Sadeghi, "Experimental Study on Vibration of Cracked Shafts using Order Analysis", Int J of Advanced Design and Manufacturing Technology, Vol. 7/ No. 2, 2014, pp. 77-87.

**Biographical notes: M. Farahmandian** is MSc student in Mechanical Engineering in East Azerbaijan Science and Research Branch, Islamic Azad University. His current research focuses on Vibration methods for fault diagnosis and condition monitoring. **M. Sadeghi** received his PhD in Mechanical Engineering from University of Michigan, Ann Arbor MI, in 1994. He is currently Associate Professor at the Department of Mechanical Engineering, Tabriz University, Iran. His current research interest includes Fault Diagnosis, Modal analysis, and FEM.

## 1 INTRODUCTION

Although modern shafts are produced for improved fatigue loading and high level of safety, using high quality materials and precision manufacturing techniques together with CAD tools, however, catastrophic failures may still occur as a result of rotor cracks. In particular, in high-speed rotating machinery with massive elements, like carrier disc rotors, impellers, gears, etc., this problem is of a great importance. Therefore, a scheme is needed to diagnose the system in the early stages and prevent breakdown. Many researches are focused on the shaft model and dynamic response of a cracked rotor.

A number of researchers have employed theoretical methods, whereas, others have combined both theoretical and experimental ones, and a few have concentrated on only experimental methods. Huang et al. investigated the dynamic response of a rotor model with a transverse crack, by obtaining the governing equations and solving them numerically [1]. He investigated the frequency response of the shaft model with different crack depths and locations, and showed that the 1X and 2X harmonics were excited. Luo et al.. set up a dynamic model for rotor bearing system with rub-impact fault coupled with cracks [2].

The results showed that there are unique dynamic characteristics of rotor bearing system with cracks coupled with rub-impact fault which are different from the ones with only one type of fault. Zheng studied the numerical vibration of rotor systems with switching cracks [3]. His use of other features of 1X and 2X harmonics were proposed for crack detection. Wen et al. studied dynamic characteristics of a rotor system with rub-impact fault coupled with the cracks, in which the effect of the imbalance, crack angle, and rotor to stator clearance were also considered in the model [4]. Wan studied vibration of a cracked rotor sliding bearing system with rotor-stator rubbing by using harmonic wavelet transform (HWT) [5]. Grabowski studied vibration behaviour of a turbine rotor having a transverse crack by using modal analysis based on geometric modelling [6]. He reported that the cracks excite 1X and 2X vibration harmonics, which are independent of the imbalance, but depend on the location of the cracks.

Darpe presented a novel way to detect transverse fatigue cracks in rotating shafts [7]. He used wavelet analysis method to exhibit the transient characteristics of the resonant bending vibrations, excited by a short-period transient torsional vibration. Dimarogonas and Paipetis developed the relationship between the depth of cracks and rotor local flexibility [8]. Meng and Hahn studied a cracked Jeffcott rotor theoretically and numerically [9]. Imam et al. used finite element method and a nonlinear rotor dynamics to model the cracked rotor system and cracked rotor fault detection which led to developing an on-line monitoring system [10]. They applied histogram signature analysis, together with Fast Fourier Transform (FFT) to distinguish between the vibration signals of un-cracked and cracked shafts. The results showed 1X and 2X vibration peaks.

Wauer performed a comprehensive review of the technical literature relating to the cracked rotor dynamics [11], [12]. He also modelled and formulated dynamic equations of cracked rotor for extensional and torsional cases. Collins et al. studied cracked rotor by modelling the shaft as a Timoshenko beam and solved six coupled equations which were obtained by Wauer [13]. They studied frequency spectrum of rotor response to the periodic axis impact. The results showed that there is an increase in the amplitude of axial, lateral and torsion vibration due to the crack. Inagaki et al. used repetitive numerical computing methods (transformation matrix) to analyze the transverse vibrations of a cracked shaft [14].

They showed that 1X and 2X vibration harmonics are present under mutual influences between gravity, imbalance and the vibration mode features at the rotating speed. They also took advantage of an experiment to validate the obtained results. Mayes and Davies analyzed the response of a multi-bearing rotor system with a transverse crack using a linear rotor dynamics computer program [15]. The result was investigated with experimental work using laboratory equipment to study the effect of the dynamic bending moment and rotor rotational speed, on crack depth.

Dirr and Schmalhorst used different methods of measuring fatigue cracks to study the effect of crack geometry with different depths on the measured vibration signals during crack propagation in a rotating shaft [16]. Fast Fourier Transform (FFT) of the experimental vibration signals, indicated the 1X and 2X vibration harmonics. Finite element model of crack was used to study bending stress distributions near the crack. Theoretical and experimental study of on-line crack detection method for rotor turbo generator was provided by Diana et al., in which the effect of thermal gradient on detection program was calculated using probability assessment [17]. The difference between the current and preceding vibration level was used to calculate vibration forces. 1X and 2X vibration frequency component was reported.

Bently and Bosmans studied experimental model for a cracked rotor of reactor coolant pump [18]. The results showed that changes in the harmonic vibration amplitude 2X and two-loop circuit is due to the crack propagation. Damarogonas and Papadopoulas studied cracked rotor stability in the coupled vibration modes [19]. Frequency spectrum of 300 MW steam turbine vibration signals revealed the vibration components with high range, and ¼ X, ½ X and 2X harmonics

indicating the deepness of cracks. Ma et al. evaluated two strong nonlinearity factors in the shaft system via experimental testing, as cracks coupled with rub-impact fault [20]. They combined concentric cascade frequency diagrams, wavelet analysis, path rotor, and the frequency spectrum, to achieve characteristics of cracks coupled with rub-impact fault, in both speed up and slow down cases.

Chan et al. showed that cracks in shafts can be identified by additional harmonics arise in the frequency spectrum [21]. The frequency of these harmonics are approximately one-half or one-third of the resonant frequency (natural frequency of the rotor) which comes up in the critical speed of the shaft. Therefore presence of these harmonics in the frequency spectrum could be an indication of cracks in the shaft. Jean investigated the use of 2X and 3X super-harmonic components for detecting the presence of a single transverse crack in a non-linear rotor system [22]. Tlaisi et al. holistically modelled the propeller-bearing-shaft system using FE procedure with the actual in-situ profiles for the propeller, bearings, supports and torque loading aluminum arm [23].

Philip et al. designed a test rig for mechanical face seal contact to detect the presence of a transverse shaft fatigue crack [24]. Experimental results of the magnitude of the 2X harmonic tilt response are provided for cracks between 0% and 40% depth. Jean-Jacques et al. presented an extension of the use of Harmonic Balance Method in the stochastic domain using the Polynomial Chaos Expansion to calculate the random non-linear dynamical response of mechanical systems [25]. They applied the proposed methodology to investigate the effects of the presence of a transverse crack in a rotating shaft under uncertain physical parameters in order to outline some robust indicators for detecting damage in rotating system.

The majority of results showed that the crack caused 1X and 2X harmonics and mainly 2X. However, imbalances may cause 1X harmonics and misalignment, asymmetry, and loosening of nuts and bolts can also produce 2X vibration harmonics. Similarly, changing in the critical speed of a rotating machine may be caused by other errors like looseness and wear. Thus, in accordance with the suggestion of Zheng, more than one feature to describe cracks in the rotor vibration should be used to avoid misdiagnosis [3].

In this study the order analysis method is employed for crack detection-isolation in a rotating shaft. The paper continues as following: In the next section the order analysis method is briefly described. In section three, the theory of modeling and simulation of cracked shafts is studied. In shaft modeling, the dynamic equations for the healthy and cracked shafts are obtained and then the codes are written in the MATLAB software environment. In section four, the test setup as well as the experimental work with different shafts with various crack depth are described. In the third and fourth step the results of different diagrams are presented for both theoretical and experimental studies. These diagrams are Frequency Spectrum Cascades that contains information about the frequency and duration of the vibration signals, Contour Plot that contains information about the environmental and structural frequencies and Order Spectrum Plot that contains information about the orders of vibration. Finally in the fifth section, discussion and conclusion are presented.

## 2 ORDER ANALYSIS METHOD

Order analysis method (OAM) is known extensively and used in troubleshooting of gears, fans, and turbines. In this research it was determined that the OAM method to be used for cracked shafts. Applying OAM method reveals any fault type of the shaft as a special order with unique features. Furthermore, this method is able to distinguish structure natural frequencies of environmental frequencies. Therefore similar to the findings of other researchers, the crack increases 2X harmonic peaks, where order analysis reveals practically this result by exciting second-order. Thus OAM method is more effective to crack troubleshooting of the shaft than other methods.

Order analysis is a form of frequency analysis that transforms the signal from the time domain to a scale based on multiples of the system driven frequency rather than absolute frequency. It is particularly advantageous for machine condition monitoring applications since it enables the orders to be tracked even while the primary frequency changes, which is generally a shortcoming of joint time-frequency analysis. During frequency changes, such as during the ramp-up or shake-down of rotating or reciprocating machinery, short-term Fourier Transform tends to spread the fundamental frequency and its harmonics, thereby providing poor resolution of the signal composition [26].

Frequency and Order analysis, are similar but with different independent arguments. Frequency analysis applies Fourier transform to a vibration signal digitised with a uniform sampling time interval ($\Delta t$), where the resulting spectrum's independent variable is in Hz. Order analysis applies Fourier transform to a vibration signal sampled on the basis of a uniform angular shaft rotation increment ($\Delta\theta$). The independent spectral variable is in orders, or multiples of shaft running speed. Order analysis has proven to be effective to track vibration components in relation to variation in running speeds [27].

## 3 THEORETICAL STUDY, MODELING AND SIMULATION OF CRACKED SHAFT AND DISCUSSION

Mathematics is the language of physical and mechanical phenomena, therefore, before the experiments are carried out, it is necessary to study the theory of mathematical modelling and numerical simulation of cracked shafts. Figure 1(a) shows schematic configuration of the shaft with a transverse crack. Figure 1(b) show cut view of cracked shaft in both fixed coordinates (X, Y), and rotating coordinates (ξ, η) and the direction which the shaft is strong, and also the direction which the shaft is weak due to crack. Shaft is rotated through a flexible coupling y the electric motor where shaft bearings are prevented from lateral movement.

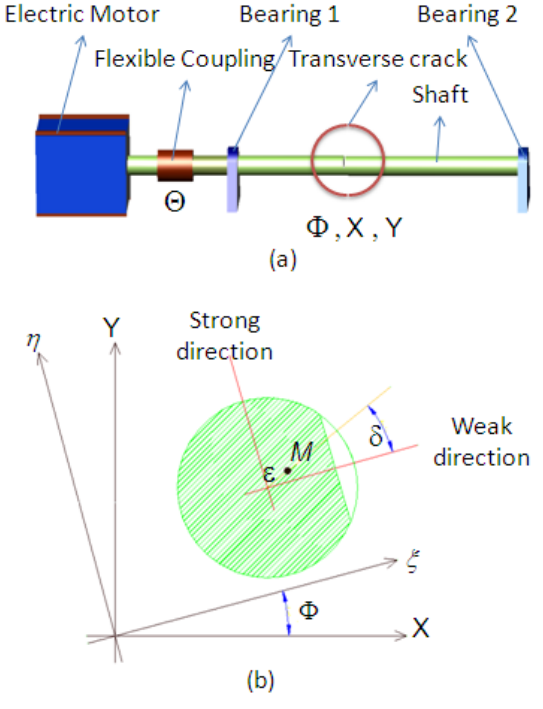


**Fig. 1** (a) Schematic configuration of shaft system, (b) Schematic cutting view of cracked shaft

A transverse crack is modelled with vertical and horizontal displacement Y and X, respectively, and the angular position, Φ(t). Similarly, angular position of the flexible coupling is shown with Θ(t). To obtain the equations of motion, dynamic equations presented in [28, 29] references are used. Bending and torsional vibrations are modelled using four degrees of freedom. Torsional rotation is located at flexible coupling and shaft crack, where lateral motion is only at the crack location.

A torque exerted on the flexible coupling via electric motor, and a downward constant radial force (p) that is located near the crack are applied to the system. Damping with lumped viscous damping due to the crack, and lumped viscous damping of the shaft are modelled. General equations of motion are obtained using Lagrange's equations expressed as follows. For the cracked shaft, equations of motion become:

$$X'' + 2\zeta X' + (1 - q\cos 2\Phi)X - q(Y_m - \frac{P}{M\omega_n^2})\sin 2\Phi = \varepsilon(\frac{\Omega}{\omega_n} + \varphi')^2 \cos(\Phi + \delta) + \varepsilon\varphi''\sin(\Phi + \delta). \quad (1)$$

$$Y_m'' + 2\zeta Y_m' - qX\sin 2\Phi + (1 + q\cos 2\Phi)Y_m = \varepsilon(\frac{\Omega}{\omega_n} + \varphi')^2 \sin(\Phi + \delta) - \varepsilon\varphi''\cos(\Phi + \delta) + \frac{P}{M}\frac{q}{\omega_n^2}\cos 2\Phi. \quad (2)$$

$$\theta'' + R_I(1 + K_r)(\frac{\omega_t}{\omega_n})^2\theta - R_I(\frac{\omega_t}{\omega_n})^2\varphi = -2R_I\zeta_t(1 + C_r)\frac{\omega_t}{\omega_n}\theta' + 2R_I\zeta_t\frac{\omega_t}{\omega_n}\varphi'. \quad (3)$$

$$\varphi'' + 2\zeta_t\frac{\omega_t}{\omega_n}\varphi' - 2\zeta_t\frac{\omega_t}{\omega_n}\theta' + (\frac{\omega_t}{\omega_n})^2\varphi - (\frac{\omega_t}{\omega_n})^2\theta = (\frac{P}{M})^2\frac{q}{\omega_n^4\rho^2}\sin 2\Phi - \frac{P}{M}\frac{q\varepsilon}{\omega_n^2\rho^2}\cos(\Phi - \delta) + \frac{\Gamma_c}{\omega_n^2}. \quad (4)$$

$$\frac{\Gamma_c}{\omega_n^2} = -2\zeta\frac{\varepsilon}{\rho^2}[X'\sin(\Phi + \delta) - Y_m'\cos(\Phi + \delta)] + \frac{\varepsilon}{\rho^2}[-X\sin(\Phi + \delta) + Y_m\cos(\Phi + \delta)] + \frac{q\varepsilon}{\rho^2}[-X\sin(\Phi - \delta) + Y_m\cos(\Phi - \delta)] - \frac{PqY_m}{M\rho^2\omega_n^2}\sin 2\Phi + \frac{q}{\rho^2}[Y_m(Y_m - \frac{P}{M\omega_n^2}) - X^2]\sin 2\Phi + \frac{2qX}{\rho^2}(Y_m - \frac{P}{M\omega_n^2})\cos 2\Phi. \quad (5)$$

Equations of motion for cracked shaft become:

$$X'' + 2\zeta X' + (1 - \frac{f(\Phi)}{2}(\Delta k_1 + \Delta k_2\cos 2\Phi)]X - \frac{f(\Phi)\Delta k_2\sin 2\Phi}{2}(Y_m - \frac{P}{M\omega_n^2}) = \varepsilon(\frac{\Omega}{\omega_n} + \varphi')^2\cos(\Phi + \delta) + \varepsilon\varphi''\sin(\Phi + \delta). \quad (6)$$

$$Y_m'' + 2\zeta Y_m' - \frac{f(\Phi)\Delta k_2 \sin 2\Phi}{2} X + [1 - \frac{f(\Phi)}{2}(\Delta k_1 - \Delta k_2 \cos 2\Phi)]Y_m = \varepsilon(\frac{\Omega}{\omega_n} + \varphi')^2 \sin(\Phi + \delta) - \varepsilon\varphi'' \cos(\Phi + \delta) - \frac{P}{M}\frac{f(\Phi)}{2\omega_n^2}(\Delta k_1 - \Delta k_2 \cos 2\Phi). \quad (7)$$

$$\theta'' + R_I(1 + K_r)(\frac{\omega_t}{\omega_n})^2\theta - R_I(\frac{\omega_t}{\omega_n})^2\varphi = -2R_I\zeta_t(1 + C_r)\frac{\omega_t}{\omega_n}\theta' + 2R_I\zeta_t\frac{\omega_t}{\omega_n}\varphi'. \quad (8)$$

$$\varphi'' + 2\zeta_t\frac{\omega_t}{\omega_n}\varphi' - 2\zeta_t\frac{\omega_t}{\omega_n}\theta' + (\frac{\omega_t}{\omega_n})^2\varphi - (\frac{\omega_t}{\omega_n})^2\theta = \frac{P}{2M}\frac{\varepsilon f(\Phi)}{\omega_n^2\rho^2}(\Delta k_1 \cos(\Phi + \delta) - \Delta k_2 \cos(\Phi - \delta)) + \frac{P^2}{2M^2}\frac{1}{\omega_n^4\rho^2}[\frac{1}{2}\frac{\partial f(\Phi)}{\partial\Phi}(\Delta k_1 - \Delta k_2 \cos 2\Phi) + f(\Phi)\Delta k_2 \sin 2\Phi] + \frac{\Gamma_c}{\omega_n^2}. \quad (9)$$

Where:

$$\frac{\Gamma_c}{\omega_n^2} = -2\zeta\frac{\varepsilon}{\rho^2}[X'\sin(\Phi + \delta) - Y_m'\cos(\Phi + \delta)] + \frac{\varepsilon}{\rho^2}(1 - \frac{f(\Phi)}{2}\Delta k_1) \times [-X\sin(\Phi + \delta) + Y_m\cos(\Phi + \delta)] + \frac{\varepsilon f(\Phi)\Delta k_2}{2\rho^2}[-X\sin(\Phi - \delta) + Y_m\cos(\Phi - \delta)] + \frac{X^2}{2\rho^2}[\frac{1}{2}\frac{\partial f(\Phi)}{\partial\Phi}(\Delta k_1 + \Delta k_2\cos 2\Phi) - f(\Phi)\Delta k_2 \sin 2\Phi] + \frac{Y_m}{2\rho^2}(Y_m - \frac{2P}{M\omega_n^2}) \times [\frac{1}{2}\frac{\partial f(\Phi)}{\partial\Phi}(\Delta k_1 - \Delta k_2\cos 2\Phi) + f(\Phi)\Delta k_2 \sin 2\Phi + \frac{\Delta k_2 X}{2\rho^2}(Y_m - \frac{P}{M\omega_n^2}) \times [\frac{\partial f(\Phi)}{\partial\Phi}\sin 2\Phi + 2f(\Phi)\cos 2\Phi]. \quad (10)$$

$$K_c = K_r K_t, C_c = C_r C_t, R_I = I/I_0. \quad (11)$$

In the above equations $Y = Y_m - P/K$ is used to delineate the static offset from dynamic response. The results of computer simulations are shown in Figures 2 to 7. The physical parameters in Table 1 are used for un-cracked and cracked shaft equations of motion [29]. Responses to un-cracked shaft are calculated from equations 1 to 5 and are shown in Figures 2, 4 and 6. Responses to the cracked shaft are calculated from equations 6 to 10 and are shown in Figures 3, 5 and 7.

**Table 1** Physical parameters of the model for the shaft vibrations

| Cracked shaft | | | Un cracked shaft | | |
|---|---|---|---|---|---|
| Parameters | Values | Units | Parameters | Values | Units |
| $\varepsilon$ | $5.08 \times 10^{-5}$ | m | $\varepsilon$ | $5.08 \times 10^{-8}$ | m |
| $\rho$ | 0.0229 | m | $\rho$ | 0.0229 | m |
| $P/M$ | 101.6 | $m/s^2$ | $P/M$ | 101.6 | $m/s^2$ |
| $\zeta_t$ | 0.02 | | $\zeta_t$ | 0.02 | |
| $\zeta$ | 0.1 | | $\zeta$ | 0.1 | |
| $K_r$ | 5 | | $K_r$ | 5 | |
| $C_r$ | 1 | | $C_r$ | 1 | |
| $\Delta k_\xi/k$ | 0.38 | | $q$ | 0.18 | |
| $\delta$ | 0 | rad | $\delta$ | 0 | rad |

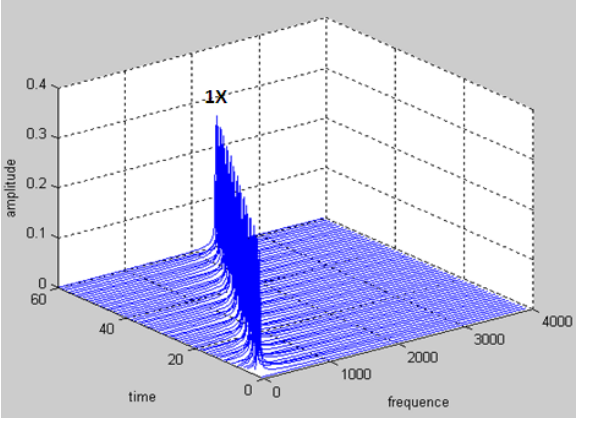


**Fig. 2** Frequency Spectrum Cascades of un-cracked shaft

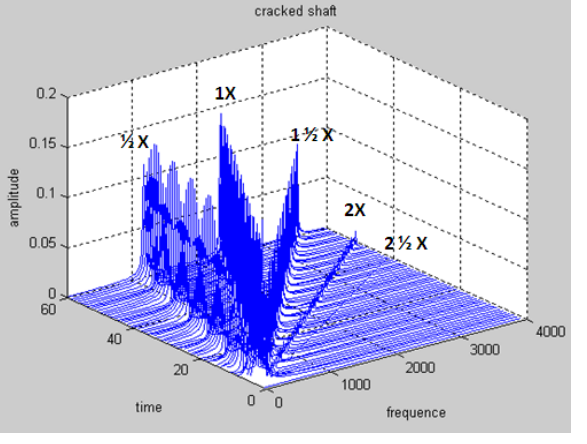


**Fig. 3** Frequency Spectrum Cascades of cracked shaft

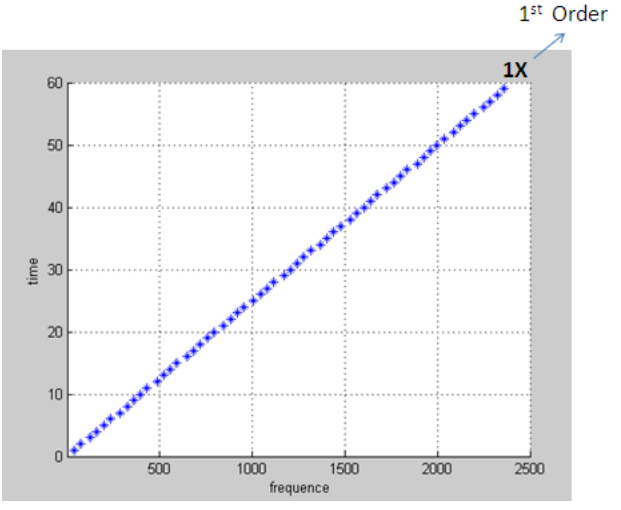


**Fig. 4** Contour plot diagram of un cracked shaft

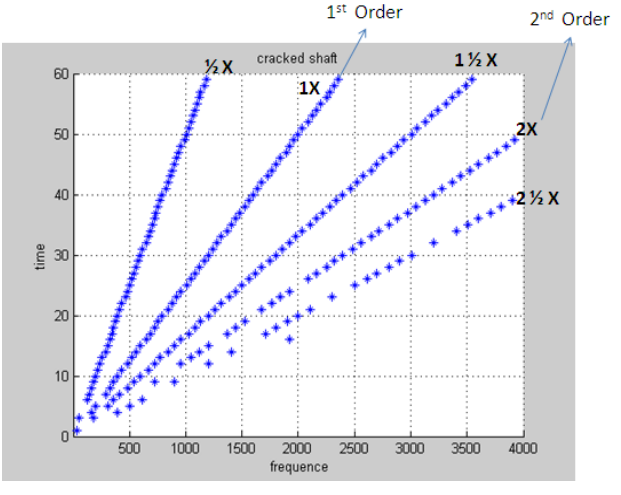


**Fig. 5** Contour plot diagram of cracked shaft

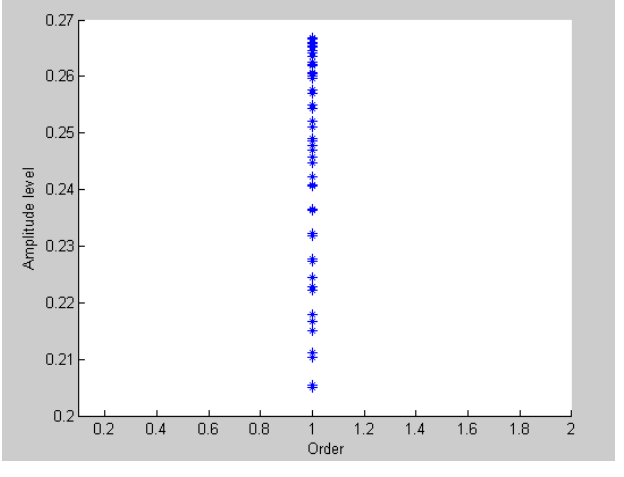


**Fig. 6** Order spectrum plot of un cracked shaft

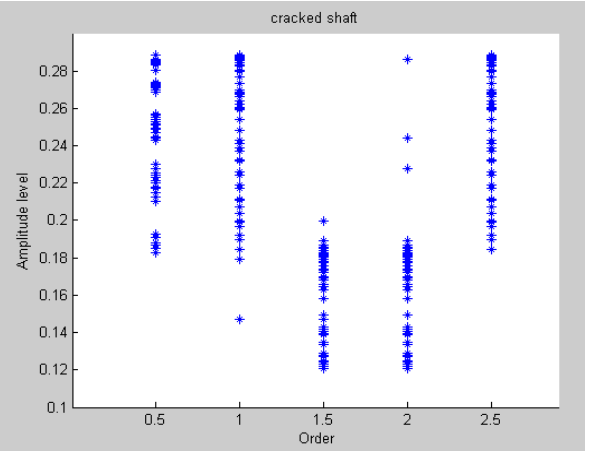


**Fig. 7** Order spectrum plot of cracked shaft

In this section the mathematical model and dynamical equations of rotating shafts are obtained. As can be seen, the analysis of the cracked shaft, leads to non-linear dynamic equations. The associated graphs were plotted by applying order Analysis method, and selecting the physical parameters of the mathematical model as close as possible to the real shaft.

Comparing healthy and cracked shaft diagrams indicates that crack in the shafts might be detected through creation or rising additional orders in the Order Spectrum Plot. Nonlinear effect of crack on the order of RPM function excites second order peaks (2nd Order), and ½ based fractional order such as ½ X (or ½ Order), 1½ Order and 2½ Order as long as rotational speed is changed. These vibration signs may be used for crack detection in shafts with variable rotational speed. These results match properly with experimental tests results.

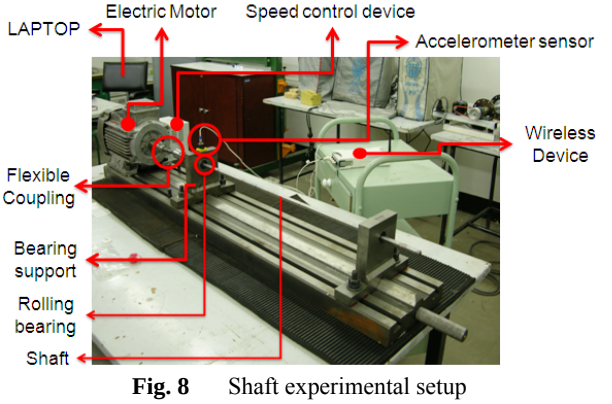


**Fig. 8** Shaft experimental setup

## 4 EXPERIMENTAL SETUP, PERFORMED EXPERIMENTAL TESTS AND DISCUSSION

In this section, experimental tests for troubleshooting of cracked shafts are studied. First, the experimental setup and measuring data equipment are explained, followed

by explaining the experimental tests procedure. Experimental setup is shown in Fig. 8, which consists of stainless steel shaft, flexible couplings, electric motor, measuring data unit (accelerometer ENDEVCO MODEL 61 C12 S / N 10837) with accessories, speed control device model SV015ic5-1, PC to collect and process data (LAPTOP), and 9163 wireless device module NI92.33. Data capturing and data processing equipment is Drive System LABVIEW, installed on Windows operating system.

Shaft dimensions and properties are, 10 mm diameter, 800 mm length, 0.61 gr/mm mass per unit length, and Young's module of 207 GPa. The distance between crack and motor bearing is 227 mm and the distance between both bearings is 570 mm, where crack depth is 40% of shaft diameter. Figure 9 shows a view of the transverse crack created in the shaft.

**Fig. 9** Transverse crack like fault made on the shaft

Motor and shaft were coupled with a flexible coupling to reduce the motor effects in the shaft system. Vibration signals were measured using vibration sensor probe fixed on the bearing support. This sensor was connected to the wireless data acquisition device through the auxiliary cable. After filtering (anti-alias filtering) and converting analog to digital (A/D), vibration signals are sent to the computer for storage and subsequent processing via Wireless devices. Several codes were developed in the MATLAB™ environment for data processing. The key point for correct analysis was the simultaneous measurement of the rotational speed of the shaft, and the vibration signal of the bearings; from the very beginning of the operation, i.e., start of the shaft from the rest.

Since each spectrum is tagged with an actual RPM, diagrams of waterfall plot and contour plot of the vibration spectrum may be shown as a function of RPM. Oblique lines with the same origin appear in the waterfall diagram, meaning that orders are functions of RPM, hence order spectrum diagram is achieved. Fast Fourier Transform (FFT) was used to transform signals from time domain to frequency domain, where principle for this purpose is the Fourier Integral, as presented below:

$$\int_{-\infty}^{\infty} X(t)\, e^{-j2\pi ft}\, dt \qquad (12)$$

It should be explained, that according to Nyquist theory the reconstruction of the original signal from its sampled data is possible only if fS>2fN, where fS is the sampling frequency and fN is the highest frequency component of the original signal. Otherwise a phenomenon called Aliasing will occur, resulting not only to have totally misrepresentative sampled data, but also to lose the original signal. To neutralize these adverse effects, all the frequency components of the original signal which are greater than half of the sampling frequency must be attenuated. This is done by an analog-to-digital converter (A/D) using a low pass filter which is called anti alias filter. The aforementioned signal process is the basic and the most major step applied on the continuous time signal.

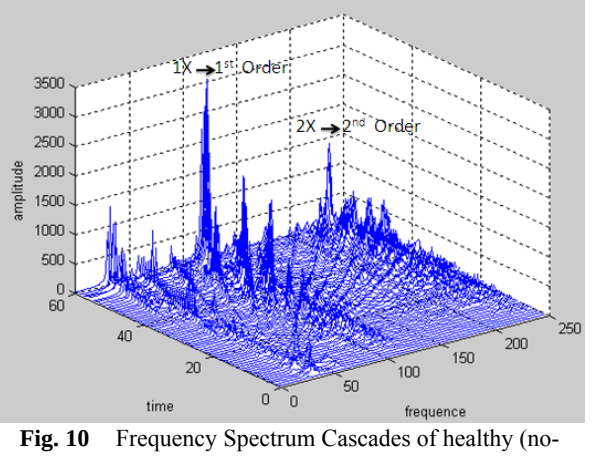


**Fig. 10** Frequency Spectrum Cascades of healthy (no-crack) shaft

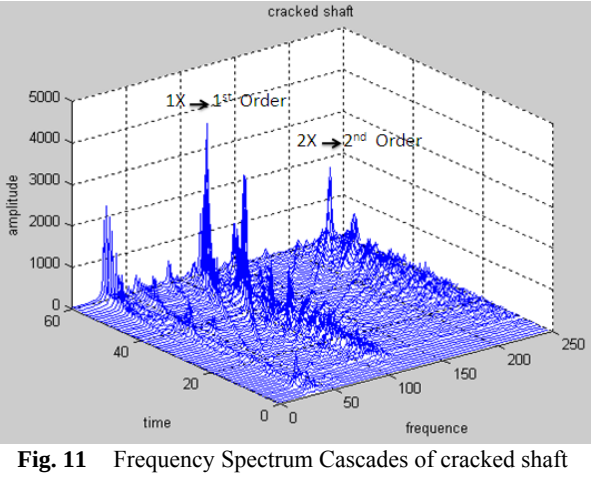


**Fig. 11** Frequency Spectrum Cascades of cracked shaft

Experimental tests were carried out on cracked and healthy shaft, where the sampling frequency was 1024 Hz and duration of data acquisition for each test was 60 seconds. During each test the motor rotational speed increased gradually from zero to 1800 rpm. It is noted that cracks with depths less than 20%, resulted in

similar response to healthy shaft, therefore were excluded from being considered. The experimental results and order analysis application are described as follows.

Figures 10 and 11 show Frequency Spectrum Cascades for cracked and healthy shafts. These figures indicate that cracked shaft vibration amplitudes were increased relative to the healthy shaft one. To obtain these figures, fast Fourier transform (FFT) were performed by writing a code in MATLAB environment. It is also observed that the vibration harmonics of the healthy and cracked shaft varies with increasing rotational speed, being functions of RPM. As a result, frequencies directions change on the diagrams obliquely with the same origin.

These RPM functions mean Orders. On the other hand, some of the harmonics generated in the shaft, are not function of the shaft rotational speed, and are constant. Therefore, directions of these frequencies on the diagrams change parallel to the time axis. This means that these harmonics are in fact consistent with the structural resonance frequencies of the shafts. In order to make figures 10 and 11 more clear, figures 12 and 13 are reproduced, highlighting the order lines and the resonance frequency lines. Comparing figures 10 and 11 (or figures 12 and 13) it is observed that the crack causes the critical speed to be reduced.

Correspondingly, first critical speed of healthy shaft is 1750 RPM, while first critical speed of cracked shaft is 1590 RPM. Furthermore, it is clearly seen that crack excites 1X and 2X vibration harmonics, and according to order analysis method, crack failure causes an increase in amplitude of first and second orders. These are features that might be trusted to identify shaft cracks, which are consistent with theoretical studies.

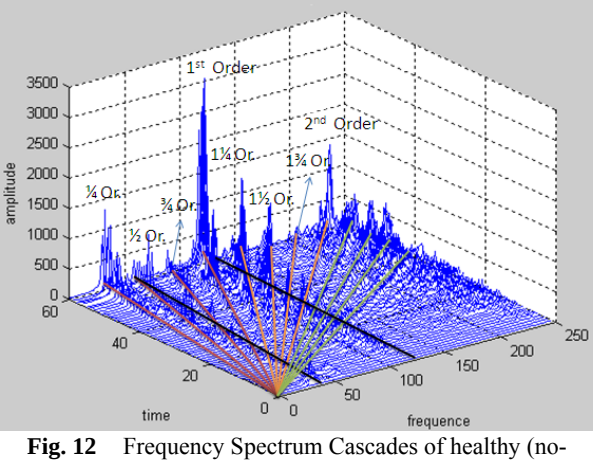


**Fig. 12** Frequency Spectrum Cascades of healthy (no-crack) shaft

Figures 14 and 15 show Contour Plot of healthy and cracked shafts. In these figures, the results of order analysis method are presented clearly, and orders that are functions of RPM where frequencies directions change on the diagrams obliquely with the same origin, have become more visible than figures 10 and 11. Moreover, first structural resonance frequency direction change parallel to the time axis (marked with the orange line). With more in depth consideration of both cracked and healthy shaft diagrams, it is observed that where the range of 2nd order is defined, harmonics of cracked shaft diagrams are richer than healthy shaft diagrams.

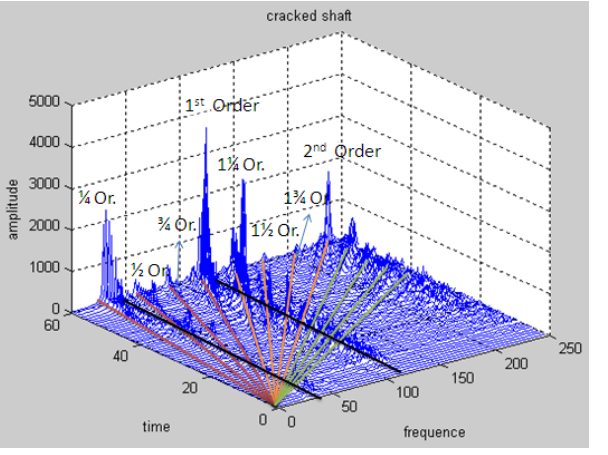


**Fig. 13** Frequency Spectrum Cascades of cracked shaft

In fact, it can be concluded that in the cracked shaft failure the extra order have been appeared. The presented results are in good agreement with previous results by others, but it is apparent that the present method displays these results more clearly. Nonetheless, it is seen that experimental results are in agreement with theoretical results, where nonlinear effects of crack excites 2nd Order and ½ based fractional orders such as ½, 1½ and 2 ½ Order as long as rotational speed is changed.

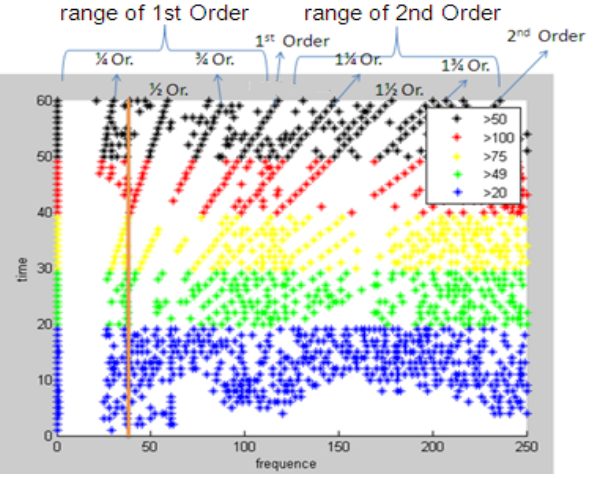


**Fig. 14** Contour Plot Diagram of healthy (no-crack) shaft

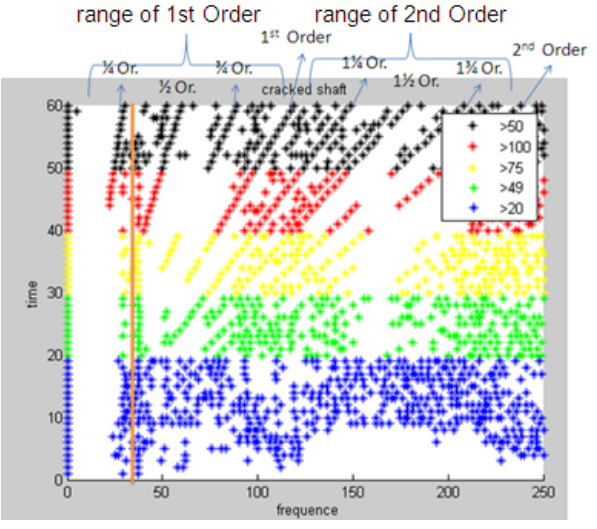


**Fig. 15** Contour Plot Diagram of cracked shaft

Considering the experimental test diagrams against theoretical diagrams of healthy shaft, it is noted that there are some orders. This is due to an unwanted imbalance fault in flexible couplings, so producing these orders in the range of 1st order. Moreover, misalignment and bearing looseness produced orders in the range of 2nd order. Figure guide is added in the upper right corner of Figures 14 and 15 to show increasing and decreasing of order amplitudes (measurement scale is arbitrary).

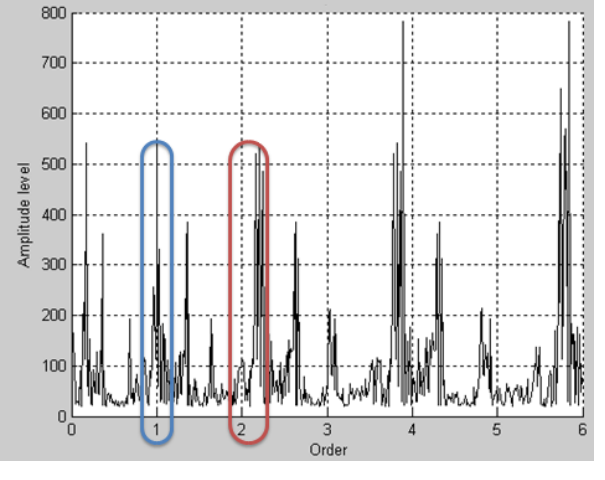


**Fig. 16** Order Spectrum Plot of un cracked shaft

Investigating the above diagrams it is found that order analysis method for troubleshooting the cracked shaft is a powerful and reliable method. The results of order analysis method are presented in Figs. 16 and 17 with Order Spectrum Plot of healthy and cracked shaft, respectively. First order is specified with blue closed line, and second order with red closed line. Comparing both diagrams, iy is concluded that cracks cause first and second order excitation, and in particular the second order. This feature may be applied for detecting cracks in shafts via order analysis method.

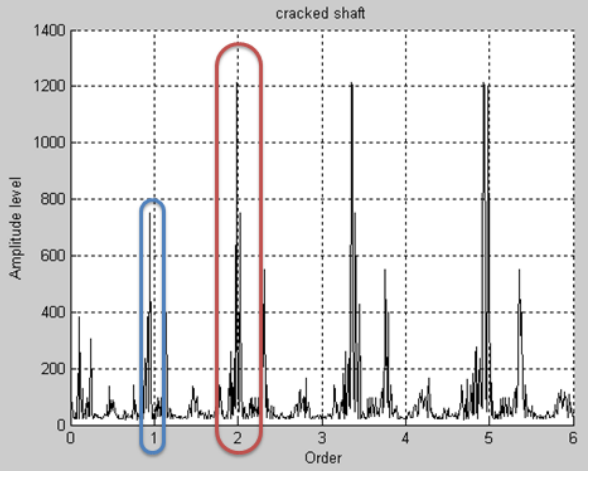


**Fig. 17** Order Spectrum Plot of cracked shaft

## 5 CONCLUSION

In this research, the capability of order analysis in detection of crack failure in shaft is demonstrated. At the first stage, this capability was shown via a simulation; in which a numerical model was created to study and analyze orders of vibration signals resulting from mathematical model. Then experimental tests were performed to investigate Order Analysis method from technical point of view, having industrial applications and also verify theoretical results. The results show that order analysis method based on the vibration signals obtained from the bearings is a good and trustable tool for detecting cracks in the shaft. Order Analysis method is well suited to identify crack in shaft with the following features. It is able to distinguish between the natural frequencies and environment frequencies from other sources. As a result, crack effects on natural frequencies can be highlighted easily, by showing a decrease in the shaft's natural frequency. In addition, by the order analysis technique, the first and second vibration orders arises in the crack failure are seen more clearly which is in perfect agreement with other researchers result.

## 6 LIST OF SYMBOLS

| | |
|---|---|
| $\omega_n$ , $\omega_t$ | The lateral and torsional natural frequency |
| $\Theta$ | Flexible coupling angle position |
| $\theta$ | Angular displacement of the flexible coupling to engine |

| | |
|---|---|
| $\theta_0$ | The initial angular position of the flexible coupling |
| $\Phi$ | The angular position of the crack |
| $\varphi$ | Crack angular displacement relative to the engine |
| $\varphi_0$ | The initial angular position of crack |
| $I_0$ , I | Respectively polar moment of inertia of shaft and flexible couplings |
| $\delta$ | The angular orientation of crack cross-section eccentricity |
| $\Gamma_c$ | Auxiliary terms in the crack equations of motion |
| M | Mass of the shaft |
| P | Vertical side load |
| X , Y | Lateral movement of crack, in the fixed coordinates |
| $K_r$ | Hardness ratio: Kc / Kt |
| $C_r$ | Damping ratio: $C_c$ / $C_t$ |
| $R_I$ | Polar momentum of inertia ratio: $I/I_0$ |
| $\xi$ , $\eta$ | Rotational coordinates fixed on the shaft |
| $Y_m$ | Dynamic vertical vibrations in the fixed coordinates |
| $\varepsilon$ | Eccentricity of crack cross section |
| $\Omega$ | Engine speed |
| $C_c$ , $K_c$ | Respectively, Damping and stiffness of motor-shaft coupling |
| C , $C_t$ | Damping coefficient of Respectively lateral and torsional |
| $\zeta$ , $\zeta_t$ | Damping ratio of Respectively lateral and torsional |
| $K_t$ | Torsional stiffness of the shaft |
| K | Shaft stiffness in healthy |
| $K_{Ic}$ | Stiffness matrix of cracked shaft in the a fixed coordinate |
| $K_{Ih}$ | Healthy shaft stiffness matrix in the a fixed coordinate |
| $K_R$ | Healthy shaft stiffness matrix in the rotating coordinate |
| $F(\Phi)$ | Crack steering function |
| $\rho$ | Radius of gyration |
| $\Delta k_\xi$ , $\Delta k_\eta$ | Reduced stiffness, respectively in the direction of $\xi$ , $\eta$ |
| q | Stiffness Factor |

## ACKNOWLEDGMENTS

The authors appreciate the support provided by University of East Azerbaijan Science and Research Branch, Islamic Azad University, Tabriz, Iran.

## REFERENCES

[1] Huang, S. S., Wu, M. C., "In-Plane vibration and crack detection of a rotating shaft disk containing a transverse crack", Journal of Vibration and Acoustics 120, 1998, pp. 551-555.

[2] Luo, Y. G., Ren, Z. H., Ma, H., Yu, T., and Wen, B. C., "Stability of periodic motion the rotor-bearing system with coupling faults of crack and rub-impact", Journal of Mechanical Science and Technology, Vol. 21, No. 6, 2007, pp. 860-864.

[3] Zheng, G. T., "Vibration of a rotor system with a switching crack and detection of the crack", Journal of Engineering for Gas Turbine, Vol. 120, 1998, pp. 149-154.

[4] Wen, B. C., Wu, X. H., and Ding, Q., et al., "Theory and experiment of nonlinear dynamics for rotating machinery with faults", Science Press, Being, 2004, pp. 112-124 (in Chinese).

[5] Wan, F. Y., Xu, Y. Q., and Li, S. T., "Vibration analysis of cracked rotor sliding bearing system with rotor-stator rubbing by harmonic wavelet transform", Journal of Sound and Vibration, Vol. 271, 2004, pp. 507-518.

[6] Grabowski, B., "The vibration behavior of a turbine rotor-containing a transverse crack", Transactions of the ASME, Vol. 102, 1980, pp. 141-146.

[7] Darpe, A. K., "A novel way to detect transverse surface crack in a rotating shaft", Journal of Sound and Vibration, Vol. 305, 2007, pp. 151-171.

[8] Dimarogonas, A. D., Paipetis, S. A., "Analytical methods in rotor dynamics", Applied Science Publishers, London, 1983.

[9] Meng, G., Hahn, E. J., "Dynamic response of a cracked rotor with some comments on crack detection", Journal of Engineering for Gas Turbine, Vol. 119, 1997, pp. 447-455.

[10] Imam, S. H., Azzaro, R. J., Bankert, D. and Scheibel, J., "Development of an on-line rotor crack detection and monitoring system", Journal of Vibration, Acoustics, Stress, and Reliability in Design, Vol. 111, 1989, pp. 241-250.

[11] Wauer, J., "On the dynamics of cracked rotors: A literature survey", Applied Mechanics Review, Vol. 43, No. 1, 1990, pp. 13-17.

[12] Wauer, J. "Modeling and formulation of equations of motion for cracked rotating shafts", International Journal of Solids Structures, Vol. 26, No. 8, 1990, pp. 901-914.

[13] Collins, K. R., Plaut, R. H., Via, C. E., and Wauer, J., "Detection of cracks in rotating timoshenko shafts using axial impulses", Transactions of the ASME, Vol. 113, 1991, pp. 74-78.

[14] Inagaki, T., Kanki, H., and Shiraki, S., "Transverse vibrations of a general cracked rotor bearing system", Journal of Mechanical Design, Vol. 104, 1982, pp. 345-355.

[15] Mayes, I. W., Davies, W. G. R., "Analysis of the response of a multi-rotor-bearing system containing a transverse crack in a rotor", Journal of Vibration, Acoustics, Stress, and Reliability in Design, Vol. 106, 1984, pp. 139-145.

[16] Dirr, B. O., chmalhorst, B. K., "Crack depth analysis of a rotating shaft by vibration measurements", 11th ASME

Conference on Mechanical Vibration and Noise, Boston, 1987, pp. 607-614.

[17] Diana, G., Bachschmid, N., and Angeli, F., "An on-line crack detection method for turbogenerator rotors", Proceedings of International Conference on Rotordynamics, Tokyo, 1986, pp. 385-390.

[18] Bently, D. E., Bosmans, R. F., "Case study of shaft crack failure, orbit", 1989.

[19] Damarogonas, A. D., Papadopoulas, C. A., "Vibration of cracked shaft in bending," Journal of Sound and Vibration, Vol. 91, 1983, pp. 583-593.

[20] Ma, H., Yu, T., et al., "Time–frequency features of two types of coupled rub-impact faults in rotor systems," Journal of Sound and Vibration, Vol. 321, 2009, pp. 1109-1128.

[21] Chan, R. K. C., Lai, T. C., "Digital simulation of a rotating shaft with a transverse crack", Applied Mathematical Modelling, Vol. 19, No. 7, 1995, pp. 411-420.

[22] Jean-Jacques, S., "Detection of cracks in rotor based on the 2X and 3X super-harmonic frequency components and the crack-unbalance interactions," Laboratoire de Tribologie et Dynamique des Syst`emes UMR-CNRS 5513, Ecole Centrale de Lyon, 36 avenue Guy de Collongue, 69134 Ecully Cedex, France, 2013.

[23] Tlaisi, A., Akinturk, A., Swamidas, A. S. J., and Haddara, M. R., "Crack detection in shaft using lateral and torsional vibration measurements and analyses," Faculty of Engineering and Applied Science, Memorial University of Newfoundland, St. John's, Canada, 2012.

[24] Philip, V., Itzhak, G., "Crack detection in a rotor dynamic system by vibration monitoring-part II: extended analysis and experimental results", Journal of Engineering for Gas Turbines and Power, Woodruff School of Mechanical Engineering, Georgia Institute of Technology, Atlanta, GA, 30332, 2012.

[25] Jean-Jacques, S., Beatrice, F., "The vibration signature of chordal cracks in a rotor system including uncertainties", Laboratoire de Tribologie et Dynamique des Systèmes UMR-CNRS 5513, Ecole Centrale de Lyon, 36 avenue Guy de Collongue, 69134 Ecully Cedex, France, 2012.

[26] Whelan, M. J., Janoyan, K. D., "Development of a wireless predictive maintenance sensor network for lost foam casting," Clarkson University, Potsdam New York, 2007.

[27] Groover, Ch. L., Trethewey, M. W., "Removal of order domain content in rotating equipment signals by double resampling", Mechanical Systems and Signal Processing, 2003.

[28] Wu, X., Meagher, J., and Judd, C., "Investigation of coupled lateral and torsional vibrations of a cracked rotor under radial load", in Proceedings of the 25th International Modal Analysis Conference (IMAC '07), Society for Experimental Mechanics, Orlando, Fla, USA, February 2007.

[29] Wu, X., Meagher, J., "A two-disk extended jeffcott rotor model distinguishing a shaft crack from other rotating asymmetries", Hindawi Publishing Corporation, International Journal of Rotating Machinery, Volume 2008, Article ID 846365, 11 pages, doi:10.1155/2008/846365, 2008.